THE ASTROPHYSICAL JOURNAL, 347:294–301, 1989 December 1

THE DISTRIBUTION AND KINEMATICS OF AMMONIA IN THE ORION-KL NEBULA: HIGH-SENSITIVITY VLA MAPS OF THE $NH_3(3, 2)$ LINE

V. MIGENES
Astronomy and Astrophysics Department, University of Pennsylvania
K. J. JOHNSTON AND T. A. PAULS
E. O. Hulburt Center for Space Research, Naval Research Laboratory
AND
T. L. WILSON
Max-Planck-Institut für Radioastronomie
Received 1988 September 26; accepted 1989 April 8

ABSTRACT

VLA maps of the $(J, K) = (3, 2)$ rotation-inversion line of NH_3 toward the Orion-KL nebula show that the emission is clumped on $\approx 1''$ scales. There are 11 distinct fragments with peak intensities more than 7 times the rms noise. In seven of these fragments the line width is equal to or less than 1.3 km s^{-1}, the velocity resolution used. These widths are considerably smaller than the widths measured with single-dish radio telescopes and show that the shape of the single-dish profiles is caused by the relative motion of individual clumps. These fragments may not be stable and may be the site of low-mass star formation. Thus the present observations give a qualitatively different picture of the fragmentation process on scales of 10^{16} cm. Apparently, turbulent motions within the individual clumps are small, and most of the kinetic energy is contained in orbital motion. For VLA observations, we find that the (3, 2) line spectra agree better with spectra of other nonmetastable ($J > K$) lines than with metastable ($J = K$) lines. This confirms that the nonmetastable and metastable NH_3 lines are formed in different regions of the "hot core." Maps averaged over velocity intervals of 10 km s^{-1} and smoothed to $2''$ show that structure in the "hot core" is consistent with a clumpy cylinder whose axis is inclined at about 40° east of north and expanding at 10 km s^{-1}. Maps smoothed to $2''$ show that, in addition to the ammonia in the "hot core," there is also weak extended emission $30''$ to east.

Subject headings: interstellar: molecules — radio sources: spectra — stars: formation

I. INTRODUCTION

The ammonia molecule, NH_3, has numerous rotation-inversion $[(J, K) \rightarrow (J, K)]$ transitions at centimeter wavelengths (e.g., Townes and Schawlow 1955; Ho and Townes 1983), and 33 of these transitions have been measured with the Effelsberg 100 m radio telescope (Hermsen *et al.* 1988, which includes an energy level diagram in Fig. 1) toward the Orion-KL nebula. Most single-dish profiles are well represented by three blended, Gaussian velocity components: the narrow "spike" at about 8.6 km s^{-1} with a full width at half-maximum (FWHM) of 2–4 km s^{-1}, the "hot core" with a velocity of 5 km s^{-1} and a FWHM of 8 km s^{-1}, and the "plateau" centered at 6 km s^{-1} with a FWHM of >15 km s^{-1}. In high spatial resolution observations such a decomposition is not physically relevant. Because a large number of inversion transitions from both the ^{14}N and ^{15}N species have been measured using the 100 m telescope (Hermsen *et al.* 1985), there is a good determination of the kinetic temperature and abundance of ammonia in the "hot core." VLA maps of Orion-KL (Genzel *et al.* 1982; Pauls *et al.* 1983; Hermsen, Wilson, and Bieging 1988) also show that the most intense ammonia emission arises in the "hot core" region. This source has a diameter of approximately $10''$ and is located about $6''$ southwest of IRc2. Although the average properties of the NH_3 are well determined from single-dish spectra, gradients in ammonia in the "hot core" are not accurately known. In principle these may be estimated by comparing VLA maps of different inversion transitions. There are, however, complications. In most rotation-inversion transitions, the spectra are split by the electric quadruple moment term of the form $\{1 - [3K^2/J(J + 1)]\}$ in the Hamiltonian, of the nitrogen nucleus. Although this splitting yields many useful physical parameters, the satellite hyperfine components can coincide with the central group of hyperfine components from another velocity component, and this will confuse the already complex spectra. However, there is an accidental cancellation of the quadruple hyperfine splitting for the $(J, K) = (3, 2)$ line. In this case, the shape of the inversion line is affected only by magnetic hyperfine splitting, which is less than 7 kHz, or 0.1 km s^{-1} at the line rest frequency. For this reason, maps in the $(J, K) = (3, 2)$ line are particularly useful for tracing the motions in the molecular gas. A map in the (3, 2) line has the added advantage that the quadruple split hyperfine components are absent, so that different velocity features can be unambiguously identified. On the other hand, because of the lack of hyperfine satellite lines, no estimates of the optical depth of the (3, 2) inversion line are possible. The best fit to a large collection of single-dish data from Orion-KL is given by model 4 of Hermsen *et al.* (1988). In this model, the optical depth of the (3, 2) line is 6. The (3, 2) energy levels are populated mostly by the absorption of far-IR continuum radiation from warm dust. Details of the model are given in Hermsen *et al.* (1988).

Analysis of previous VLA maps indicated that structure was present on scales of $\leq 1''$ (Pauls *et al.* 1983; Hermsen, Wilson, and Bieging 1988). However, the arguments used were indirect and higher angular resolution maps are needed. Such high-resolution maps of thermally excited spectral lines require much higher sensitivity than previous measurements. Recently,

two technical improvements have become available: (1) it is possible to carry out line observations with 25 antennas, rather than the 13 antenna configurations used by Genzel *et al.* (1982) or Pauls *et al.* (1983), and (2) a number of VLA antennas have been equipped with more sensitive receivers. These improvements allow a factor of 3 improvement in sensitivity, and this encouraged us to reobserve the $(J, K) = (3, 2)$ rotation-inversion line in Orion-KL.

II. OBSERVATIONS

The (3, 2) rotation-inversion transition of ammonia was observed on January 4 1987 using 25 antennas in the C-configuration of the Very Large Array of the National Radio Astronomy Observatory[1] The observations were made with a total bandwidth of 3.125 MHz divided into 32 contiguous channels. The data were Hanning-smoothed, on-line. The spectral resolution was 1.3 km s^{-1} centered at a radial velocity of 8.0 km s^{-1} relative to the local standard of rest (LSR). A full 10 hr synthesis was made by alternately observing the calibrator, 0528+134, for 5 minutes and Orion-KL, at R.A. (1950) = $05^h32^m46^s.8$ and decl. (1950) = $-05°24'22''$, for 8 minutes. The flux density scale was established by assuming a flux density for 3C 84 of 42.0 Jy at 22.834 GHz. The data on 0528+134 were used to determine the instrumental amplitude and phases. The channel with the strongest emission was cleaned and used to self-calibrate the *u-v* data. The *u-v* data were Fourier transformed using natural weighting and the maps were cleaned, using 300 iterations, with a cellsize of 0".3 on a 256 × 256 grid. The rms noise of a single channel map is 5 mJy (= 9 K, T_B). The synthesized half-power beam width is 1".24 × 1".20 at a position angle of 41° east of north.

III. RESULTS

a) *Average Profile and Terminology*

In Figure 1, we show a spectrum of the $NH_3(3, 2)$ transition toward the Orion-KL region obtained on 1986 October 26 with the Effelsberg telescope (Hermsen *et al.* 1988). The spectral resolution is 0.64 km s^{-1}. The rest frequency of the line is 22834.185 MHz and the velocities are relative to the LSR. The full width to zero-power (FWZP) of this line is more than 50 km s^{-1}.

Single-dish NH_3 profiles consist of a number of blended velocity components. A conventional analysis using Gaussian line shapes shows that three velocity features are needed to provide an adequate fit (see Hermsen *et al.* 1988). We give the V_{LSR} and FWHM of the various velocity components in Figure 1. The "spike" component has a line width of less than 2 km s^{-1}, and in order to even marginaly resolve this feature, a velocity resolution of 1.3 km s^{-1} is required. We chose this value because we also wanted the highest sensitivity possible and, therefore, used 25 antennas of the VLA. Because of restrictions imposed by VLA software, the maximum number of spectral channels was 32, which limited the maximum velocity coverage to 42 km s^{-1}. This velocity range is shown as a bar below the profile in Figure 1.

b) *Extensive Clumping Present*

There is considerable small-scale structure on the maps with full (≈1".2) resolution. In Figure 2 gray-scale plots of individual spectral channels are overlaid on the average NH_3 contours and show the location of numerous fragments, or clumps found on the maps at 4.2–8.0 km s^{-1}. We have identified at least 11 such fragments on our maps with peak intensities greater than 35 mJy, but only four have widths extending over several velocity channels. As a comparison, in Figure 4 we show the gray-scale plot for 17 km s^{-1}; here only two weak maxima can be seen at the same levels used in Figure 2. Parameters for these fragments are given in Table 1. The peak flux density of the fragments are at least 7 times the rms noise in the maps and stand out quite well, as an inspection of Figure 2 shows. In fact, the number of fragments increases dramatically if we reduce the cutoff intensity. Gaussians have been fitted to these fragments to estimate their size. However, note that the shapes of these fragments are very irregular. Therefore, the Gaussian sizes are only very rough estimates of the dimensions of the fragments. The line widths in Table 1 have not been corrected for the 1.3 km s^{-1} resolution of the spectrometer. In seven cases, the individual fragments have linewidths which are equal to or less than this resolution. One can easily see from Figure 2 that the fragments do *not* occur in adjacent channels. For a kinetic temperature of 160 K, as estimated from NH_3 data (Hermsen *et al.* 1988), the line width would be 0.8 km s^{-1},

[1] Operated by Associated Universities, Inc., under cooperative agreement with the National Science Foundation.

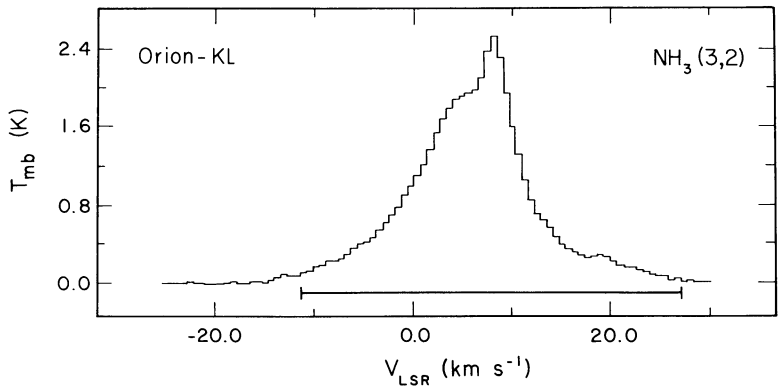

FIG. 1.—Spectrum of the $NH_3(3, 2)$ line toward the Orion-KL nebula taken with the Effelsberg 100 m radio telescope which has an angular resolution of 43" at a frequency of 23 GHz. The horizontal bar represents the bandpass of the VLA used for the observations reported in this paper. A three-component nonlinear least-squares fit to the line yields the following estimates for the parameters (Hermsen *et al.* 1988). The strong, narrow "spike" component has a radial velocity of 8.7 km s^{-1}, width of 2.6 km s^{-1}, and T_B = 9.6 K, the "hot core" component has a radial velocity of 5.6 km s^{-1}, width of 8.8 km s^{-1} and T_B = 4.8 K, and the weak, broad "plateau" component has a radial velocity of ~6 km s^{-1}, a width of ~20 km s^{-1} and T_B = ~1 K.

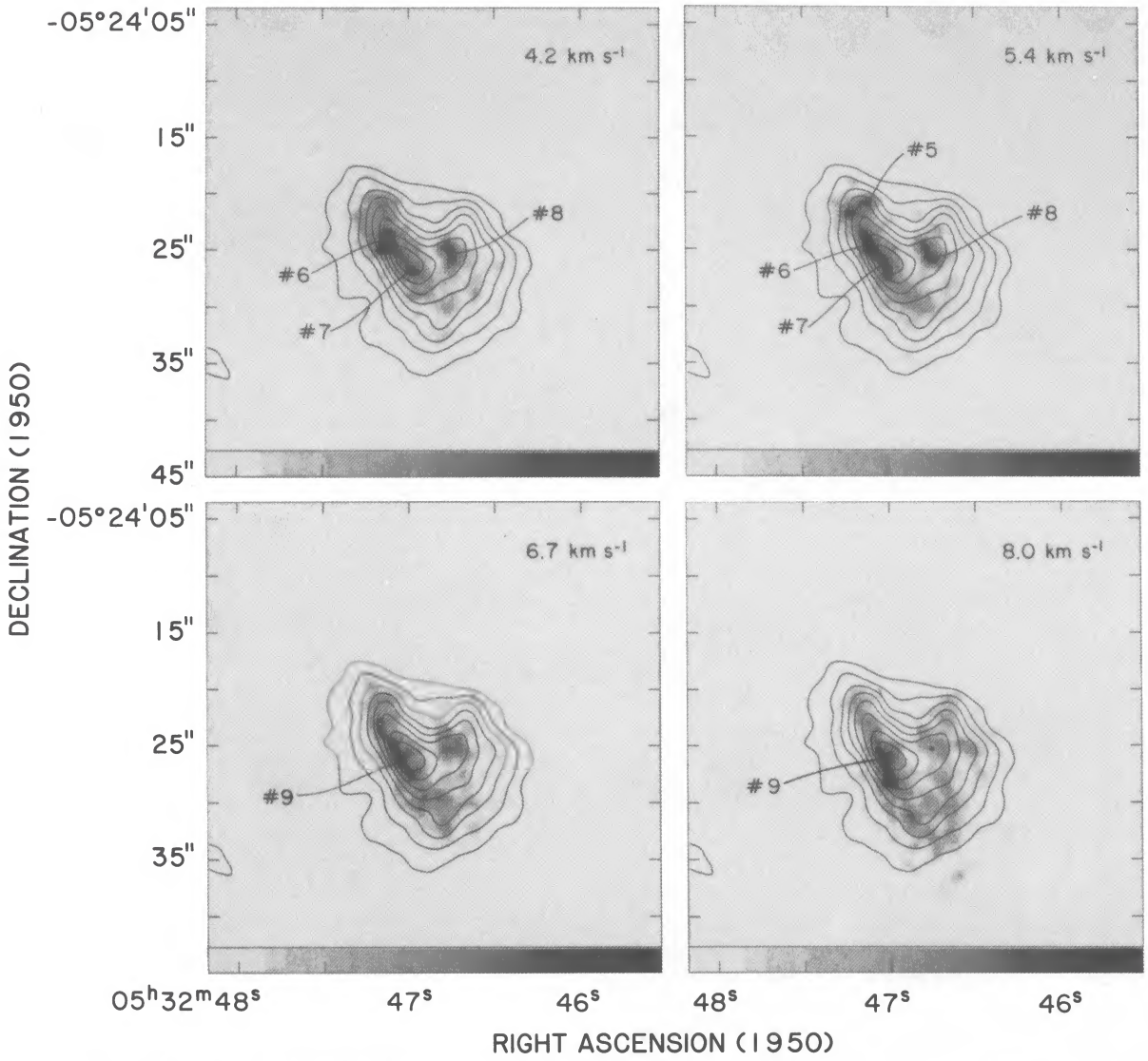

FIG. 2.—VLA maps of the NH_3 individual line channels for radial velocities between $V_{LSR} = 4.2$ and 8.0 km s^{-1} are shown on a gray scale. The intensity range of the gray-scale maps is 15–60 mJy beam^{-1}, the spatial resolution is 1".24 × 1".21 at a position angle of −41°, and the spectral resolution is 1.3 km s^{-1}. The approximate locations of several clumps in Table 1 are indicated. The contours are the average over VLA maps covering radial velocities −11.2 to 27.2 km s^{-1} and smoothed to 2". The contour intervals are 20, 30, 40, 50, 60, 70, 80, 90% of the peak intensity 55 mJy beam^{-1} (= 32.5 K, T_B in a 2" beam).

so that at our velocity resolution, we cannot determine whether there are supersonic or subsonic motions in each clump. The virial mass and density estimates in Table 1 were made using the formulae found in the Appendix of the paper by Batrla *et al.* (1983). For the narrow-line sources, these estimates are upper limits. It should also be pointed out that these masses and densities are only rough estimates since the spatial sizes for the fragments are based upon the assumption these are Gaussian-shaped. Also because of possible interactions with outflowing material, virial estimates may not be relevant, since the line widths may not represent the equilibrium of kinetic and gravitational energy alone.

c) *Extended Emission East of the "Hot Core"*

We made the maps in Figure 3 by first averaging the individual channel maps in a given velocity interval, and then smoothing the resulting map to a spatial resolution of 2". A striking feature in Figure 3 is the presence of extended emission 30" east of the ammonia "hot core." The peak intensity is low and would not have been found in previous VLA maps (Genzel *et al.* 1982; Pauls *et al.* 1983). This weak feature has a slightly different shape in the different velocity ranges, which indicates that it may be caused by spectral-line emission with a line width larger than or comparable to our total spectrometer coverage, 42 km s^{-1}. Any interpretation of this new feature is complicated by the fact that the peak intensity is the same in all velocity ranges, although the shapes differ slightly in the different velocity ranges. It is not clear whether the emission is caused by an NH_3 line of width >20 km s^{-1} or broad-band continuum. If caused by NH_3, the peak line temperature is approximately 80 K, which would indicate a hot molecular region. Even with large optical depths in NH_3, the H_2 densities

TABLE 1

PARAMETERS OF CLUMPS IN ORION KL

CLUMP NUMBER	R.A. 1950	Decl. 1950	PEAK FLUX DENSITY (mJy per beam)	V_{LSR} (km s^{-1})	$\Delta V_{1/2}$[a] (km s^{-1})	SIZE[b] max (″)	SIZE[b] min (″)	POSITION ANGLE (Degrees E of N)	MASS[c] ($M_\odot$)	$n(H_2)$[c] $\times 10^7$ cm^{-3}
1.....	05^{h}32^{m}46^s.88	−05°24′26″.5	40	−4.8	2.6	2.1	1.9	12	6.2	63
2.....	05 32 46.90	−05 24 25.9	43	−3.5	≈1.3	3.3	2.3	21	≈2.1	≈9
3.....	05 32 47.04	−05 24 24.7	51	1.6	2.6	4.8	2.5	16	10.3	22
4.....	05 32 46.86	−05 24 26.5	39	0.3	<1.3	2.7	1.6	130	<1.5	<16
5*a*.....	05 32 47.10	−05 24 21.3	40	5.4	<1.3	1.0	1.0	0	<0.7	<69
5*b*.....	05 32 47.20	−05 24 21.9	45	5.4	<1.3	<1	<1			
6.....	05 32 47.10	−05 24 25.0	62	5.4	≈1.3	6.5	2.2	26	≈2.8	≈5
7.....	05 32 47.00	−05 24 27.3	51	5.4	≈1.3	4.4	2.8	21	≈2.6	≈5
8.....	05 32 46.74	−05 24 25.9	52	5.4	2.6	3.1	2.0	34	7.8	40
9.....	05 32 47.02	−05 24 26.2	63	9.3	3.9	3.4	1.8	39	17.3	92
10.....	05 32 46.66	−05 24 22.6	39	10.6	≈1.3	5.0	1.5	24	≈2.1	≈8

[a] Includes 1.3 km s^{-1} channel width.
[b] Deconvolved sizes; the maximum uncertainties are 1″.
[c] From virial theorem (see Batrla *et al.* 1983 for relevant formulae)

needed to populate the nonmetastable levels are at least 10^5 cm^{-3}. This emission has an irregular shape, which suggests expansion, perhaps caused by an interaction with Orion A. With an expansion speed of 10 km s^{-1}, the size of about 20″ (0.05 pc at 500 pc) implies a time scale of 5000 yr.

d) Average Kinematics

The smoothed maps in Figure 3 can be used to study the average kinematics of ammonia in the "hot core." Because there is no quadruple hyperfine structure in the (3, 2) line, we can easily follow the motion of the gas. Figure 3*b*, which covers the velocity range of the "hot core" centered at ≈6 km s^{-1}, has two ridges of emission separated by 4″ (≈0.01 pc at 500 pc) at a position angle of approximately 40°. The eastern ridge has 1.5 times the intensity of the western ridge. The FWHM of the intensity of the eastern ridge is 4″. At negative velocities, there is a single peak between the two ridges (Fig. 3*a*), and at more positive velocities (Fig. 3*c*), there are also two maxima, but the intensities are about 3 times smaller, and the peak intensities of the ridges are equal. The placement of the negative velocity maximum between the two ridges suggests that the observations may be interpreted as due to an incomplete, expanding cylinder. The systemic velocity would be approximately 6 km s^{-1}, and the expansion of the near side would be about 10 km s^{-1}. There is no positive velocity counterpart, which suggests that the cylinder has an incomplete far side. The FWHM of the ridges in Figure 3*b* indicates that the cylinder-wall thickness is about one-half of the total diameter. Combined with the near-IR polarization data of Werner, Dinerstein, and Capps (1983) and the IR maps of Wynn-Williams *et al.* (1984), it would appear that the NH_3 delineates the inner boundary of the cavity around IRc2.

One objection to such a simple model is that the axis of the cylinder does not pass through the position of IRc2. This offset in position may be related to gradients in H_2 density or chemical formation/destruction processes affecting the abundance of NH_3. From size and expansion speed, the characteristic time scale is approximately 10^3 yr. This is consistent with time scales from H_2O maser proper motions (Genzel *et al.* 1981), CO outflow (e.g., Wilson, Serabyn, and Henkel 1986) and chemical dynamics (Walmsley *et al.* 1987).

IV. DISCUSSION

a) Comparison with Previous VLA Maps of NH_3

In Figure 4 we show the position of peaks A–D of Pauls *et al.* 1983) on a 2″ resolution velocity-averaged contour map. There is good agreement between peaks A–C and maxima found in our smoothed map. Toward peak D, there is less emission in the (3, 2) inversion line. However, as pointed out by Pauls *et al.* (1983), the optical depth of the (3, 3) metastable line at peak D is small, and this is a temperature, but not necessarily a column density, maximum. The small optical depth reduces the effect of photon trapping in the rotational lines of NH_3, and for a given H_2 density will reduce the population in nonmetastable levels. Hermsen, Wilson, and Bieging (1988) also found that the intensity of the nonmetastable (4, 3) line was very much less than that of the (3, 3) inversion transition at this location.

Previous detailed VLA studies of the (3, 3) and (4, 3) ammonia transition by Pauls *et al.* (1983) and Hermsen, Wilson, and Bieging (1988) analyze spectra made at four positions of enhanced emission (A–D) by averaging over 2″ × 2″ regions. Our analysis of these regions is summarized in Table 2. We see that the agreement between the radial velocities of the (4, 3) and the (3, 2) inversion lines are quite good, but the agreement with V_{LSR} of the (3, 3) line is less satisfactory. The line widths of the (3, 2) inversion lines are larger; however, the effect of optical depth on line-width has been accounted for in the case of the other lines. Peak D, farthest from IRc2, has lower temperatures in the nonmetastable lines than in the metastable line. The opposite is true for peak C closer toIRc2. There is no unique trend for peaks A and B, but the errors in the temperature scale are large. If the nonmetastable levels are populated by a far-infrared radiation field with a color temperature which exceeds the kinetic temperature, the excitation temperatures of the nonmetastable lines should be larger, if the beam-filling factors are equal. We discuss this last assumption in the next section.

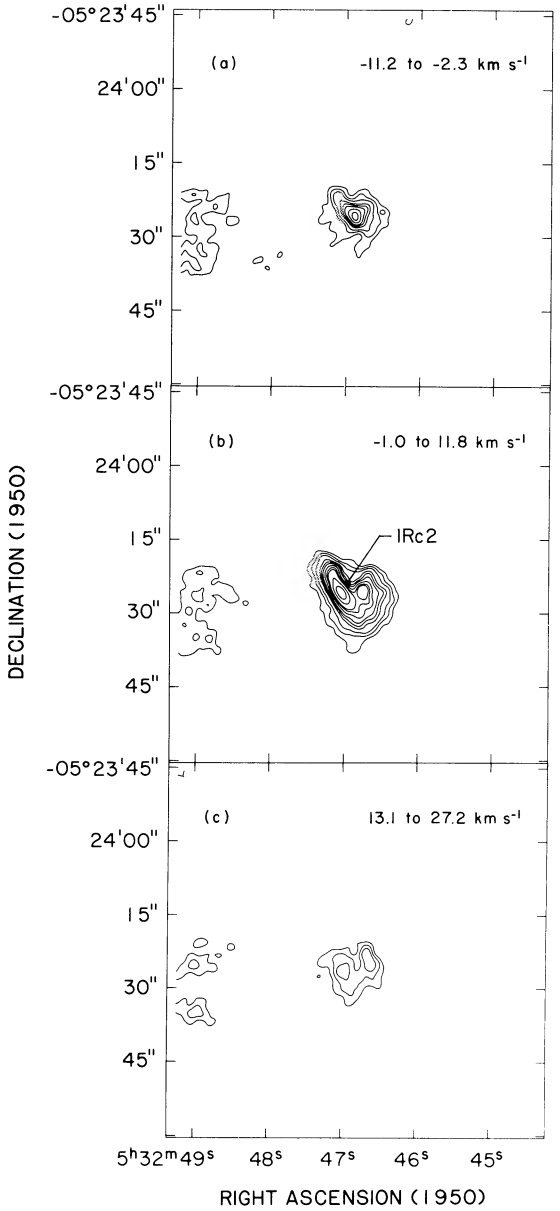

FIG. 3.—VLA maps of the $NH_3(3, 2)$ line smoothed to a resolution of 2″, from the original resolution ≈1.″2. Each map is an average over a different velocity range: (*a*) $-11.2 < V < -2.3$ km s^{-1}; (*b*) $-1.0 < V < 11.8$ km s^{-1}; (*c*) $13.1 < V < 27.2$ km s^{-1}. The values of the contour levels are 0.6, 0.8, 1.0, 1.3, 1.5, 1.7, 2.0, 2.3, 2.5, 3.0, 3.5, 4.0, and 4.5 times 25 mJy beam^{-1} (= 14.8 K, T_B in a 2″ beam).

b) Beam-filling Factors of Metastable and Nonmetastable Lines

The multiline analysis of NH_3 in Orion KL by Hermsen *et al.* (1988) shows that the peak intensity of metastable lines are larger than predicted. This shows that the volume filled by the metastable lines is larger. More compelling are our radial velocity comparisons in Table 2. All these results support the case for different spatial distributions in metastable and nonmetastable lines. Since the metastable NH_3 lines are excited at densities of 3×10^4 cm^{-3}, while nonmetastable lines require either higher densities or intense far-IR fields, it is natural that the nonmetastable lines are emitted from a smaller volume.

If so, there will be large anomalies in the formation of the rotational lines of NH_3. The detection of the (4, 3) → (3, 3) line in the far-IR by Townes *et al.* (1983) is a case in point. As noted by Hermsen *et al.* (1988), the (4, 2) → (3, 2) and (4, 1) → (3, 1) lines should also have been seen. Since the optical depths of the rotational lines should be of order 10^3, self-absorption effects may well play a decisive role. Detailed models of the KL region, including assumptions about line-of-sight geometry are needed to investigate the excitation of the rotational transitions properly.

c) The Classification of Single-Dish Profiles

The above analysis shows that the classification of single-dish spectra by means of Gaussian fits to blended components is not unique. Figure 2 shows maps of the 8.0 and 5.4 km s^{-1} velocity channels at 1.″2 resolution. The 8.0 km s^{-1} map represents mainly "spike" gas, while the 5.4 km s^{-1} map represents "hot core" material. There is no drastic difference in the appearance of these maps, aside from the fact that the "spike'. gas is more extended to the south of the "hot core." This is also the case in VLA maps of the metastable (3, 3) line (Pauls *et al.* 1983), where the appearance of the "spike" and "hot core" emission is similar. The nonmetastable (3, 2) line can be emitted only from warm gas with H_2 densities of 10^5 cm^{-3} or more. Most of the "spike" emission has smooth structure and a peak temperature of 60 K; the smooth emission would be resolved out by the VLA. Even if clumped, 60 K gas would be close to the sensitivity limit of the VLA. What we observe, then is a warmer portion of the "spike" which is heated to a higher temperature by IR sources in the KL nebula. Hermsen, Wilson, and Bieging (1988) point out that in the single-dish (6, 6) line is evidence for a hot "spike" component. Such emission may be located at the southern edge of the ammonia "hot core." This hot "spike" emission may also be related to the methanol emission center reported by Menten *et al.* (1986, 1988). There is some evidence from VLA maps of high-lying methanol lines that the methanol emission center has an embedded heat source Wilson *et al.* 1989), which may be IRc4 or IRc5.

d) The Interpretation of Single-Dish Ammonia in View of the VLA Results

In single-dish measurements with beams of 40″ or more, the NH_3 "spike" is extended north-south, while the "hot core" and "plateau" emission arise from regions small compared to the beam. In all single-dish spectra, these components have line widths which are many times the sound speed. In our VLA maps, on the other hand, there are only three regions where the line widths are at most 3–4 times the sound speed; in the remaining seven clumps, the line widths could be comparable to or less than the speed of sound for a 160 K gas. Thus the relative motion of the clumps determines the line shapes seen with a single dish. From models based on analysis of single-dish spectra, the optical depth in each of the individual clumps is probably quite large. Mauersberger *et al.* (1986) have pointed out that least-squares fits to hyperfine components in NH_3 spectra from W51 give large optical depths, but the line shapes were not consistent with saturated Gaussians. The present VLA observations show that although the optical depth of the single-dish line profiles is indeed large, the line shapes measured with a single dish are caused by the relative motion of many fragments. Thus, the line shapes are determined by the velocity distribution of the clumps and not by the emission

TABLE 2

PARAMETERS FROM PREVIOUS MEASUREMENTS OF THE "HOT CORE"

Position[a]	R.A.(1950)	Decl.(1950)	Transition	T_L (K)	$\Delta V_{1/2}$ (km s^{-1})	V_{LSR} (km s^{-1})	τ
A.....	05^{h}32^{m}46^s.7	−05°24′24″.0	(3, 3)	44±8	6.0±0.5[b]	3.3±0.4	20±5
			(4, 3)	44±5	3.0±0.3[b]	6.0±0.3	40±10
			(3, 2)	49±3	10.2±0.8[c]	6.7±0.3	
B.....	05 32 47.0	−05 24 25.0	(3, 3)	52±6	6.0±0.4[b]	5.0±0.4	20±5
			(4, 3)	70±10	3.0±0.3[b]	4.0±0.3	90±30
			(3, 2)	87±5	12.2±1.0[c]	4.3±0.3	
C.....	05 32 47.1	−05 24 21.5	(3, 3)	38±8	5.0±0.5[b]	4.1±0.3	15±5
			(4, 3)	50±5	5.0±0.3[b]	3.0±0.3	80±30
			(3, 2)	87±6	8.1±0.7[c]	4.3±0.2	
D.....	05 32 46.8	−05 24 28.0	(3, 3)	130±10	9.0 [b]	6.0	<2
			(4, 3)	35±5	6.0±1.0[b]	3.0±0.5	10±8
			(3, 2)	66±7	14.7±2.0[c]	2.8±0.6	

[a] The same letter name as used by Pauls *et al.* (1983; Table 1)
[b] Width of a single hyperfine component.
[c] Measured width of the line profile.

from an optically thick line emitted from a single region. For Orion-KL this would imply that the velocity distribution of the clumps seen in NH_3 is close to Maxwellian. The rms scatter in the radial velocities is 5 km s^{-1}, so that the relative motion of the clumps is supersonic. Applying a version of the virial theorem for star clusters (Mihalas and Routley 1968, p. 235) we obtain a mass of 70 $M_\odot$. This is more than 2 times even the largest mass estimated from high-resolution dust continuum data (Masson *et al.* 1985; Wright and Vogel 1985; and Mezger, Wink, and Zylka 1989). It is thus likely that this motion is caused in part by an interaction of the clumps in the hot core with outflows. If the NH_3 "hot core" is located in a spherical region, the relative motion and size of the clumps indicates that the mean clump-clump collision time is about 2000 yr. This may be lengthened by geometry, or by invoking soft, or grazing collisions (Scalo and Pumphrey 1982). The argument involving geometry would require that the NH_3 is located on the walls of a cavity in the KL nebula. This is consistent with the observations based on the polarization of near-IR radiation; Werner, Dinerstein, and Capps (1983) proposed such a cavity model;

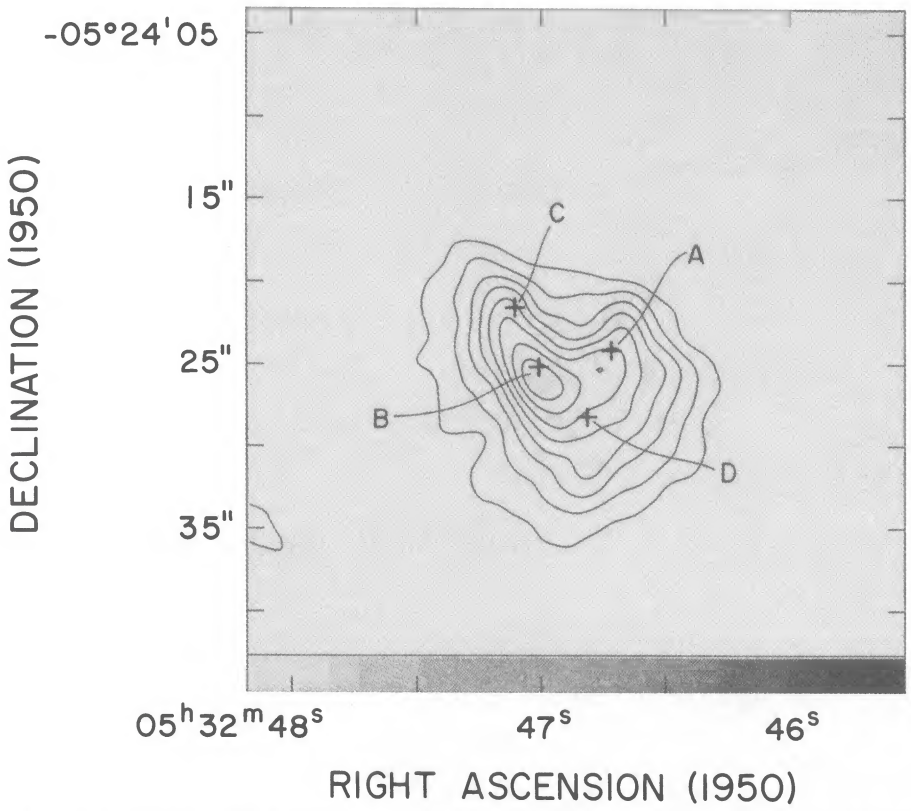

FIG. 4.—The channel map at 17 km s^{-1} plotted using the same gray scale and contour levels as in Fig. 2. The locations of the emission peaks (A–D) found in the (3, 3) (Pauls *et al.* 1983) line are indicated. Note that these positions are coincident with the overall peaks in our integrated smooth map; their relationship to the "clumps" in Table 1 is discussed in § IV*a*.

this model was later refined by Wynn-Williams *et al.* (1984). As deduced from our velocity-averaged smoothed maps (§ III*d*), the walls of such a cavity are thick, about 10^{16} cm.

e) The Ultimate Limits to VLA Measurements of Thermal Line Emission

In Table 1 we have listed only those clumps with peak intensities which are 7 times the rms noise; as the peak intensity approaches the rms noise level, the number of clumps increases dramatically. It is tempting to speculate whether there is a limit to the size and number of clumps in the ammonia "hot core." In effect, both limits are related to confusion and noise. Only variations in radial velocity allow an escape from limits set by the confusion criteria. However, the observations are ultimately limited by sensitivity, since the maximum NH_3 line temperature will be 160 K if the emission is thermal. There should be a correlation between the different channel maps when the velocity channels are separated by 0.7 km s^{-1}, the width corresponding to the sound speed (in NH_3 at 160 K). However, the present maps are still far from these limits. The total integrated line flux density for the regions listed in Table 1 is only about 30% of the single-dish value. The ultimate question is whether all of the NH_3 is contained in clumps or whether there is a smooth NH_3 medium at some level; we cannot settle this question on the basis of our data. There may be a hot interclump medium in which NH_3 cannot survive; this medium may be dominated by H I or ionized gas.

f) Implications for Star Formation

The most notable observational finding is that the line widths of the individual clumps in our VLA maps are much smaller than the widths observed with beams 2–20 times larger. The present observations give a qualitatively different picture of the fragmentation process: on scales of 10^{16} cm, the line widths in the individual clumps could be consistent with thermal broadening. Turbulence and shock waves do not dominate the motion in the individual clumps; presumably such influences must have been damped out. However, the *relative* motion of these sources is *very* supersonic. We envisage that winds from IR sources in the KL nebula and the expansion of the H II region compressed the virially stable molecular gas. This causes an increase in the H_2 density and kinetic temperature, which leads in turn to fragmentation as the molecular cloud collapses, and the angular momentum is converted into relative clump motions.

For the three regions where we resolved the lines, we can estimate virial masses and densities. From extensive analyses of single-dish data, the average H_2 density in the ammonia "hot core" is about 10^7 cm^{-3} (Hermsen *et al.* 1988). This density is a factor of 5 below upper limits to the average H_2 density in Table 1. If this density applies to these clumps, the masses in Table 1 must be lowered. From the Jeans's criterion, a spherical gas cloud having a density of 10^7 cm^{-3} and a temperature of 160 K has a limiting Jeans mass of 4 solar masses. If a clump is more massive than this, it will collapse. Density estimates, based on a measurement of the $J = 9$–8 line of HCN (Stutzki *et al.* 1988), yield a value of about 10^8 cm^{-3}. If applicable to these clumps, this value would indicate that our upper limits for the densities of seven of the regions are too small and the clumps will collapse. Additional pressure on the clumps may be provided by an interclump medium. This may be molecular or could be in the form of hot H I. If molecular, the interclump gas may be a smooth background seen as the residual after all the clumps have been removed. Any additional pressure may lead to a slow collapse, and the individual clumps would form low-mass stars.

At this density, the free-fall time is about 10^3 yr. Although this is a short time scale, the "hot core" is a small region, and time scales from other measurements (§ III*d*) are of this order. As discussed previously, although the individual clumps may be stable, there is a short time scale for clump-clump collisions. Given that the timescales for all these phenomena are of order 10^3 yr, the fragments we observe cannot be very permanent. The exact mass of stars which would form from those clumps is difficult to estimate. From the virial masses listed in Table 1, if one star is formed from each clump these stars will have masses less than 5–10 $M_\odot$. Additional fragmentation will reduce these values further, but clump-clump collisions followed by coalescence may increase the mass estimates.

IV. CONCLUSIONS

The (3, 2) inversion line maps presented here show that the sturcture of the NH_3 emission from the "hot core" is dominated by clumping even down to scales of 1″ or less. The most prominent maxima are tabulated in Table 1, but there is structure at a lower brightness temperature level. The line widths of seven of the clumps are equal to or less than the velocity resolution, 1.3 km s^{-1}. This width is considerably smaller than the widths measured with single-dish radio telescopes and shows that the shape of these profiles is caused by the relative motion of individual clumps. These clumps appear to be virially stable but clump-clump collisions may limit the lifetimes to 10^4 yr or less. Thus they may be sites of low-mass star formation.

The line widths and central velocities of spectra at selected positions show good agreement between the (3, 2) and (4, 3) inversion lines but considerably poorer agreement with the metastable (3, 3) inversion line. This supports the supposition of Hermsen *et al.* (1988) that the nonmetastable and metastable NH_3 lines are formed in different regions. Such differences could give rise to large excitation anomalies in rotational lines of NH_3. In the "hot core," the smoothed maps give some support to a model in which the NH_3 is located along the walls of a thick cylinder which is expanding at a velocity of about 10 km s^{-1}. Such a cylinder may form a part of the cavity deduced from near-IR polarization data by Werner, Dinerstein, and Capps (1983).

Smoothed maps show an irregular feature located 30″ to the east of the ammonia "hot core." From differences between averages over different velocity intervals, it appears that this feature may be caused by spectral line emission.

REFERENCES

Batrla, W., Wilson, T. L., Bastien, P., and Ruf, K. 1983, *Astr. Ap.*, **128**, 279.
Genzel, R., Downes, D., Ho, P. T. P., and Bieging J. 1982, *Ap. J. (Letters)*, **259**, L103.
Genzel, R., Reid, M., Moran, J. M., and Downes, D. 1981, *Ap. J.*, **224**, 884.
Hermsen, W., Wilson, T. L., and Bieging, J. H. 1988. *Astr. Ap.*, **201**, 276.
Hermsen. W., Wilson, T. L., Walmsley, C. M., and Batrla, W. 1985, *Astr. Ap.*, **146**, 134.
Hermsen, W., Wilson, T. L., Walmsley, C. M., and Henkel, C. 1988, *Astr. Ap.*, **201**, 285.
Ho, P. T. P., and Townes, C. H. 1983, *Ann. Rev. Astr. Ap.*, **21**, 231.
Masson, C. R., Claussen, M. J., Lo, K. Y., Moffet, A. T., Phillips, T. G., Sargent, A. I., Scott, S. L., and Scoville, N. Z. 1985, *Ap. J. (Letters)*, **295**, L47.
Mauersberger, R., Henkel, C., Wilson, T. L., and Walmsley, C. M. 1986, *Astr. Ap.*, **162**, 199.

Menten, K. M., Walmsley, C. M., Henkel, C., and Wilson, T. L. 1986, *Astr. Ap.*, **157**, 318.
——— 1988, *Astr. Ap.*, **198**, 267.
Mezger, P. G., Wink, J. E., and Zylka, R. 1989, in preparation.
Mihalas, D., and Routly, P. M. 1968, *Galactic Astronomy* (San Francisco: Freeman).
Pauls, T. A., Wilson, T. L., Bieging, J. H., and Martin, R. N. 1983, *Astr. Ap.*, **124**, 23.
Scalo, J., and Pumphrey, W. A. 1982, *Ap. J. (Letters)*, **258**, L29.
Stutzki, J., Genzel, R., and Harris, A. I. 1988, *Ap. J. (Letters)*, **330**, L125.
Townes, C. H., Genzel, R., Watson, D. M., and Storey, J. W. V. 1983, *Ap. J. (Letters)*, **269**, L11.
Townes, C. H., and Schawlow, Al L. 1955, *Microwave Spectroscopy* (New York: McGraw-Hill).
Walmsley, C. M., Hermsen, W., Henkel, C., Mauersberger, R., and Wilson, T. L. 1987, *Astr. Ap.*, **172**, 311.
Werner, M. W., Dinerstein, H. L., and Capps, R. W. 1983, *Ap. J. (Letters)*, **265**, L13.
Wilson, T. L., Serabyn, E., and Henkel, C. 1986, *Astr. Ap.*, **167**, L17.
Wilson, T. L., Johston, K. J., Henkel, C., and Menten, K. M. 1989, *Astr. Ap.*, in press.
Wright, M. C. H., and Vogel, S. N. 1985, *Ap. J. (Letters)*, **297**, L11.
Wynn-Williams, C. G., Genzel, R., Becklin, E. E., and Downes, D. 1984, *Ap. J.*, **281**, 172.

K. J. JOHNSTON and T. A. PAULS: Code 4130, Naval Research Laboratory, Washington DC 20375-5000

V. MIGENES: University of Pennsylvania, Dept. of Astronomy and Astrophysics Philadelphia, PA 19104

T. L. WILSON: Max-Planck-Institut für Radioastronomie, Auf dem Hugel 69, D-5300 Bonn 1, Federal Republic of Germany